Available online at www.sciencedirect.com
ScienceDirect
Nuclear Instruments and Methods in Physics Research A 566 (2006) 351–359
NUCLEAR INSTRUMENTS & METHODS IN PHYSICS RESEARCH Section A
www.elsevier.com/locate/nima

Photo-current scanner system for in situ quality assessment of large area CsI photocathodes

H. Hoedlmoser[a,*], A. Braem[a], G. De Cataldo[a,b], M. Davenport[a], A. Di Mauro[a], A. Franco[b], A. Gallas[b], P. Martinengo[a], E. Nappi[b], F. Piuz[a], E. Schyns[a]

[a]*CERN, Switzerland*
[b]*INFN-Sez. di Bari, Bari, Italy*

Received 10 May 2006; received in revised form 21 June 2006; accepted 25 July 2006
Available online 22 August 2006

Abstract

The facility for the production of the large area ($64 \times 42\,cm^2$) CsI photocathodes (PCs) for the ALICE/HMPID detector has been equipped with a photo-current scanner system for the in situ measurement of the CsI response over the full photo-sensitive area before transfer to the detector. This paper provides a detailed description of the experimental setup. Measurements of variations in the photo-current due to the pad structure of the PCs as well as due to heat treatment and ageing effects of the CsI PCs demonstrate the sensitivity of the instrument to changes in quantum efficiency (QE). The usability of the scanner to perform quality monitoring during the series production of PCs for the detector is shown in a comparison of scanner measurements and beam test results for 17 PCs.

PACS: 25.6; 34.8a

Keywords: CsI photocathode; Heat enhancement; Ageing; RICH; HMPID

1. Introduction

The ALICE High Momentum Particle Identification (HMPID) detector [1,2] consists of seven RICH detector modules covering a total sensitive area of $11\,m^2$. It features a proximity focusing layout in which the primary ionizing particle generates Cherenkov light inside a liquid C_6F_{14} radiator. The UV photons are converted into photo-electrons inside the 300 nm CsI coating of the PC and the photo-electrons are amplified in an avalanche process inside a Multi Wire Proportional Chamber (MWPC) with the PC acting as one of the cathodes. The detector signal is read out from the PC which is segmented into pads ($8\,mm \times 8.4\,mm$) to allow the reconstruction of the Cherenkov rings. The schematic cross-section of the detector is given in Fig. 1.

The substrate for the $64 \times 42\,cm^2$ CsI PCs is a double layer Cu clad PCB coated with Ni and Au. The 300 nm layer of CsI is deposited onto the substrate by evaporation of CsI from four crucibles under vacuum (10^{-6} mbar). The substrate temperature during evaporation is 60 °C . PCs are kept at this temperature for a minimum of 12 h after coating. Details about the PCs and the production procedures can be found in Refs. [3–5]. The current status of the ALICE HMPID project is described in Ref. [6]. In the past the PCs have been tested as integrated detectors with charged particle beams. Comparison of the test beam data with Monte Carlo predictions allows the extraction of QE data and the assessment of the PC quality [7]. As this procedure is time consuming and depending on beam availability,[1] the CsI coating plant has been equipped with a Vacuum Ultra Violet (VUV) scanner system which allows a 2D mapping of the photo-current across the PC surface immediately after the coating process and thus provides an alternative method to evaluate the PC quality. First results obtained with this VUV-scanner have been presented in

*Corresponding author.
E-mail address: herbert.hoedlmoser@cern.ch (H. Hoedlmoser).

[1]There was no test beam available at CERN in the mass production phase in 2005.

0168-9002/$ - see front matter © 2006 Elsevier B.V. All rights reserved.
doi:10.1016/j.nima.2006.07.052

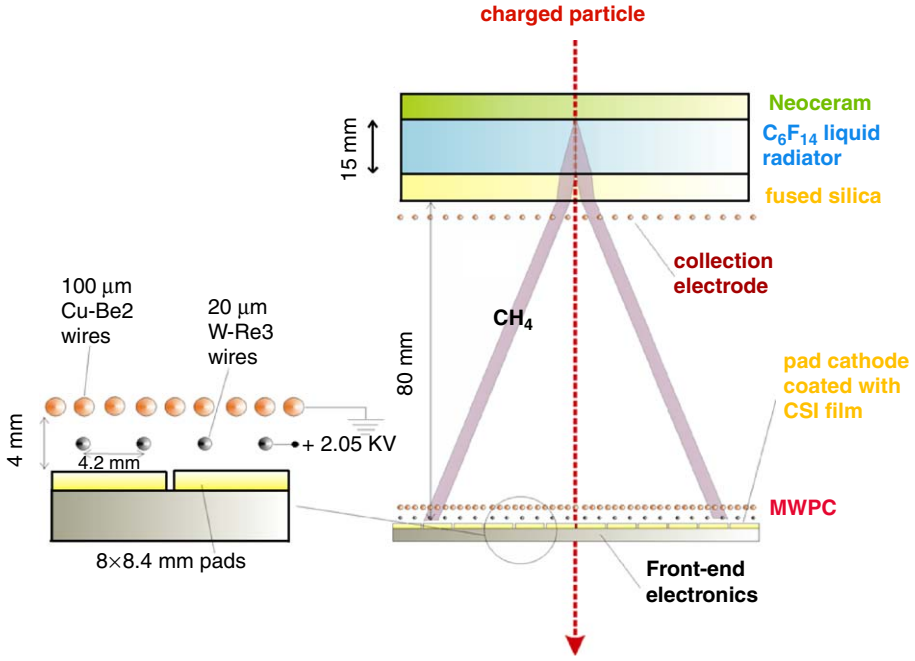

Fig. 1. Schematic drawing of the HMPID RICH detector.

Ref. [8]. This paper focuses on a detailed description of the experimental setup and of the measurement procedures including a discussion of systematic effects that have to be dealt with in these measurements, e.g. the influence of ageing under UV flux and that of the PC pad structure. Furthermore, measurements of the change in PC quality due to heat enhancement procedures or resulting from ageing tests involving ion bombardment during MWPC operation are presented to demonstrate the sensitivity of the instrument to QE variations and its performance as a research tool. A comparison of the photo-current scans on 17 PCs with beam test results provides acceptance criteria, as the scanner is currently used to monitor PC quality and homogeneity in the series production of the 42 PCs necessary to equip the HMPID detector.

2. VUV-scanner system

2.1. Experimental setup

The VUV-scanner system allows to scan the PC with a UV beam and read the resulting photo-current from a given location on the PC. Fig. 2 shows the basic layout of the measurement system.

The system outside the main chamber contains the UV lamp[2] under Ar flow and UV optics (CaF_2 lens, pinholes, diaphragm, optional quartz filter) under vacuum. This optical system is connected to the main chamber by a flexible bellow, which allows to move the optics in and out of the chamber. The volumes are separated by CaF_2 windows. In the main chamber the UV beam (adjustable between 2.5 and 16 mm diameter) is directed onto the PC via a rotatable mirror. The PC is fixed to two rails at the top of the chamber with the CsI coated pads facing downward. After the CsI coating process, the PC is moved along these rails from the CsI evaporation side to the measurement side of the vacuum vessel. The photo-electrons produced by the UV beam are extracted from the PC by means of a bias voltage of +100 V on an anode ring approximately 5 mm in front of the PC. The PC is connected to a pico-ammeter for the measurement of the photo-current (Fig. 2). By means of the mirror, the beam can be directed onto a CsI photo-multiplier[3] (PM) to obtain a reference measurement. The software controlled movements of the optical system and of the PC itself, allow a fully automated scan of the photo-current over the PC surface. The scans are performed according to a set of pre-defined coordinates, with a positioning accuracy of 1 mm.

2.2. Measurement method

For each point in a VUV-scan the photo-current I_{CsI} from the PC is recorded as well as the reference signal I_{PM} from the PM (read from the first dynode) and the background levels $I_{CsInoise}$ and $I_{PMnoise}$. The reference current on the PM is used to normalize the photo-current from the PC according to $I_{norm} = (I_{CsI} - I_{CsInoise})/(I_{PM} - I_{PMnoise})$. The currents are measured without amplification in the range of approximately 50–500 pA, whereas the background currents are <1 pA. I_{norm} has a typical value between 3 and 3.8. A repeated measurement

[2]Hamamatsu L7292 with a MgF_2 window (http://www.sales.hamamatsu.com/).

[3]Electron Tubes 9403B (http://www.electrontubes.com/).

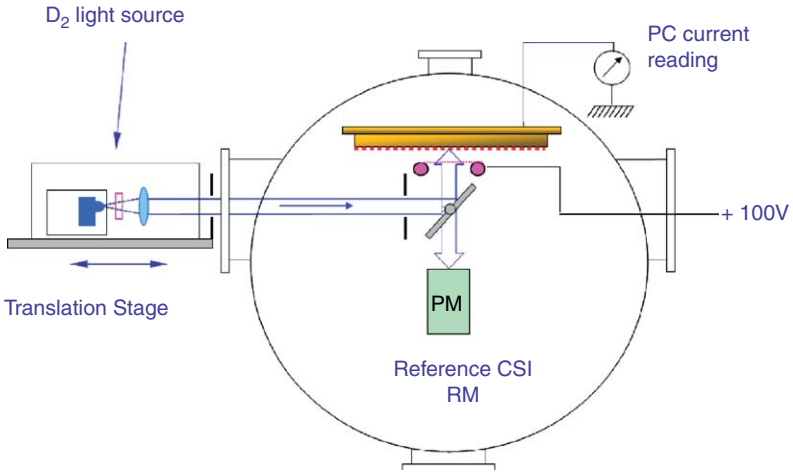

Fig. 2. VUV-scanner measurement layout.

on a single spot on a PC including repositioning of the spot shows a reproducibility of 98%.

2.3. Systematic effects

During the commissioning phase of the VUV-scanner a number of systematic effects which can influence the photo-current measurements have been identified and the experimental setup and procedures have been optimized to keep these effects under control. For a detailed description of these setup specific effects, which include the pick up of stray UV light on the large PC surface, influences of UV spot size and form, geometrical alignment problems, choice of photo-electron extraction field, influence of the measurement due to the operation of penning gauges as well as the influence of residual pressure and temperature, the reader is referred to Ref. [9]. Contrary to the above-mentioned effects, which are specific to the experimental conditions, one effect has to be mentioned here in particular as it is intrinsic to any photo-current measurement on CsI PCs: the influence of the ageing of CsI PCs under high photon flux. As there are a number of publications [10–12] reporting a degradation of the QE of CsI PCs under high photon flux, several tests were performed to ascertain that measurements in the VUV scanner have no detrimental effect on the CsI PCs. In test irradiations with doses up to 2×10^{17} photons cm^{-2} the reported effects could be confirmed, however they were found to be temporary and the irradiated PCs showed a recovery within a few days after irradiation. In the current configuration of the VUV scanner the applied photon flux is less than 2×10^{10} photons $cm^{-2}\,s^{-1}$. For this flux no degradation is observed, on the contrary, in continued measurements a non-permanent increase of the photo-current can be observed, which can be tentatively explained by an increase of the sensitivity in the long wavelength range ($\geqslant 180$ nm) in low dose irradiation as shown in Ref. [11]. For a standard mapping of a CsI PC (measurement time $\leqslant 30$ s per measured point) this non-permanent increase is less than 0.2% and can consequently be neglected. However, for other applications of the scanner involving a long time monitoring of the development of the QE of a PC (compare Section 3.2), it follows that the monitoring has to be performed in periodically repeated measurements and cannot be done in a continuous measurement on a single spot.

3. Sensitivity to QE variations and applications

In the following section several examples of measurements performed with the scanner are given, which demonstrate the sensitivity of the instrument to variations in QE and show the broad range of applications for the systems use as a research tool. In addition to providing accurate information about the QE uniformity across the PCs both on a large scale and on the level of a single pad, it was also used to measure characteristic properties of the CsI PCs both on standard large area PCs and smaller test substrates. Among the investigated phenomena are the post deposition heat enhancement effect, which has been reported for small cathode samples [2,13–15] and ageing effects of CsI PCs due to exposure to humid air and to ion bombardment.

3.1. Reduced effective QE in interpad zones

If used in a configuration with a small UV spotsize (2.5 mm diameter), the VUV scanner is able to detect variations in photo-current resulting from the pad structure of the PC. The pads on a standard PC are separated by an insulating zone of 0.5 mm width. These interpad zones account for 11% of the total area of a PC. If a UV photon extracts a photo-electron from the top of the 300 nm CsI layer on a pad, the charge can be replaced through the connection of the Au–Ni layer to ground. The electron only has to be transported through the relatively thin CsI layer (bulk resistivity: $2.8 \times 10^{10}\,\Omega$ cm [16]). If a photo-electron is extracted from the CsI layer covering the

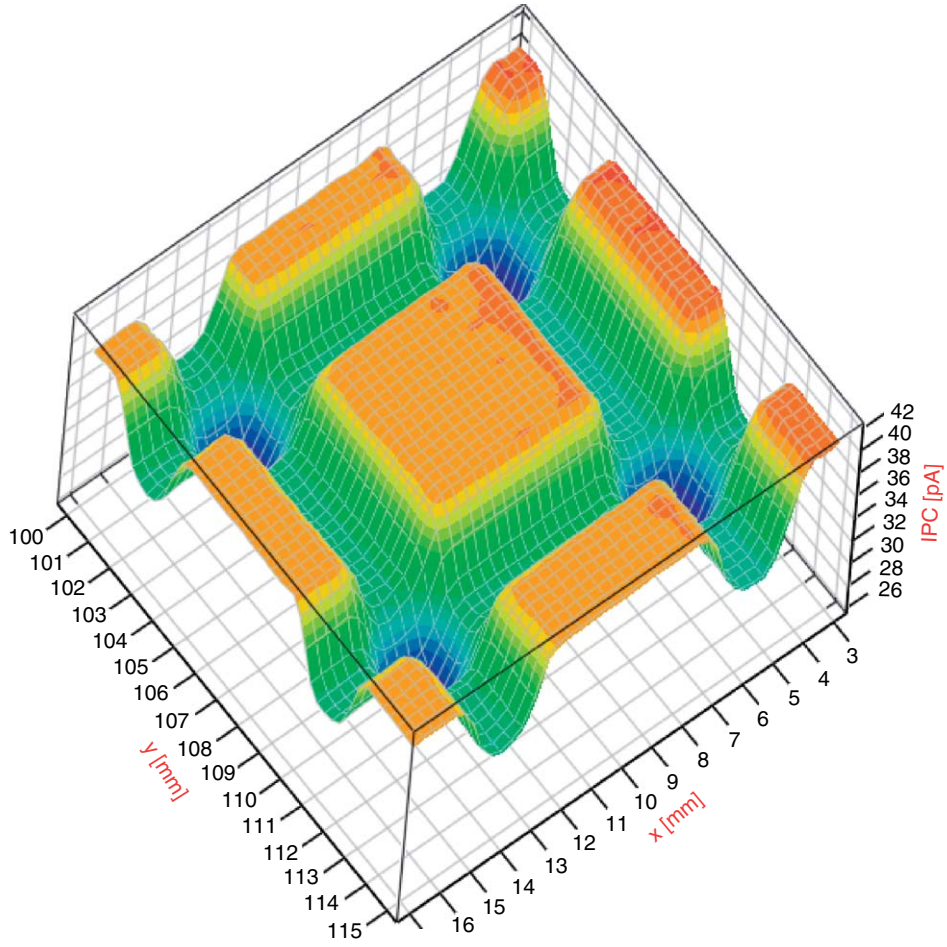

Fig. 3. Detailed scan across 2 × 2 pads of a PC showing a decreased photo-current in the inter-pad zones.

insulating interpad zone, the charge can only be replaced by a transport over a much larger distance through the CsI layer from the nearest pad. The higher resistance in the current circuit will lead to a lower effective value of the QE of CsI in the interpad zones compared to the QE on the pad. A detailed scan across 2 × 2 pads (Fig. 3) confirms the QE drop in the interpad zones, which is however less than could be expected from a calculation assuming zero QE in the interpad zone.

3.2. QE increase during heat enhancement phase

A series of CsI depositions onto a test substrate[4] was performed and the heat enhancement of the photo-current was measured both for depositions on cold (20–25 °C) and hot (65 °C) substrates. The scanner was used to continuously record the development of the photo-current immediately after CsI deposition.

Fig. 4 shows a measurement of the time development of the temperature on the PC backside and of the photo-current averaged over several points on the PC. The CsI deposition was carried out at room temperature and the initial photo-currents were low. The PC was heated first to 30 °C and afterwards to 65 °C, which caused a 50% increase of the photo-current compared to the initial level.[5] Afterwards the PC was cooled down to 25 °C and the photo-current remained at the elevated level. When the measurement was repeated three days afterwards, the current was found to be stable. Several other tests showed a similar behavior both for evaporations at 25 and at 65 °C. Usually the enhancement phase is shorter for evaporations at 65 °C with equal final results. In 20% of a total of 50 investigated CsI depositions including test substrates, the PCs did not exhibit an increase during the initial heat treatment. However those PCs, which were monitored further, showed a very slow increase of the photo-current during several weeks after production—see Section 4.1.

3.3. Comparative measurements on substrate samples

The VUV scanner also provides a means to compare the performance of different types of substrates. It is possible to mount several test substrates of varying size on an Al support plate which replaces the standard PC substrate. All

[4] 27 × 39 cm^2 test substrate identical to the standard PC substrates, except it was not segmented into pads.

[5] The increase depends on the spectrum used in the measurement.

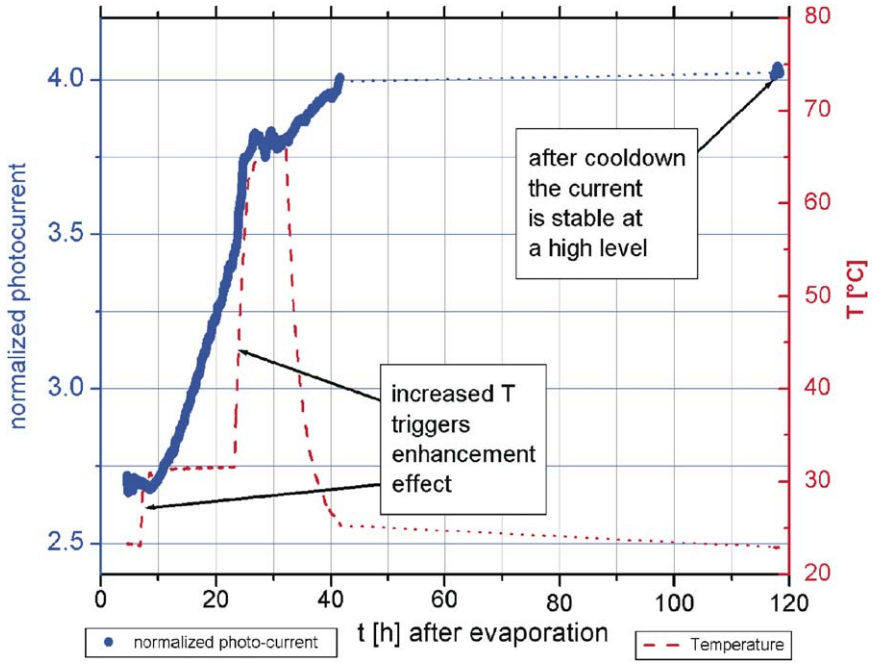

Fig. 4. Time development of $\langle I_{\mathrm{norm}} \rangle$ and T during heat enhancement phase.

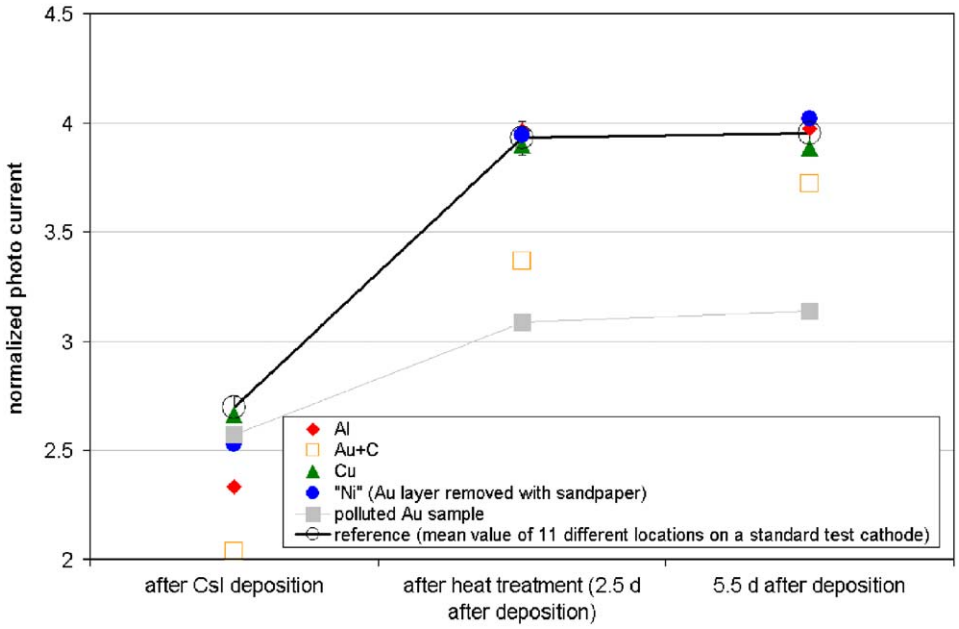

Fig. 5. Comparison of the performance of different types of substrates coated in the same process. (Process details: evaporation at 25 °C, heating to 35 °C after 7 h, heating to 75 °C after 23 h, cooldown to room temperature after 32 h.)

the substrates are then coated in a single evaporation procedure which allows a direct comparison of samples produced under identical coating conditions. Fig. 5 shows a comparison between several types of substrates and a standard PCB substrate. Except for a polluted sample and a carbon coated Au-substrate, all the substrates show a similar behavior during and after the enhancement phase.

3.4. Exposure to humidity

As indicated in Fig. 6, the test PC described in Section 3.2 was exposed to air in the clean room facility 145 h after CsI deposition. The exposure lasted for 4 h at a relative humidity of 15% at 22 °C. Humidity is known to destroy the hygroscopic CsI film, e.g. Ref. [13] and references therein. Subsequently, the vacuum chamber was closed,

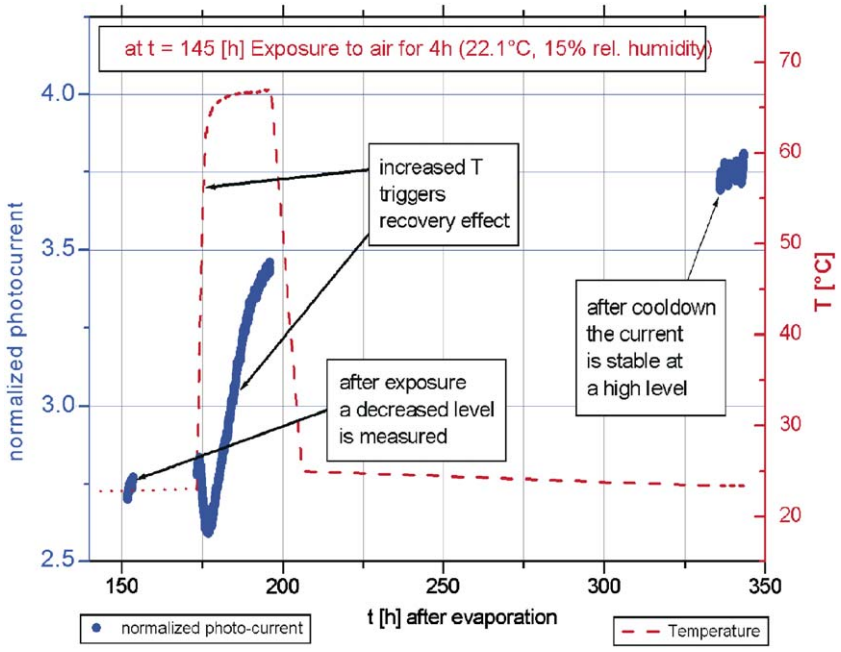

Fig. 6. Time development of $\langle I_{\mathrm{norm}} \rangle$ and T after exposure to humid air (extension of Fig. 4).

pumped again and the measurement restarted. The photo-current was decreased by 31% compared to the level before exposure. Twenty four hours later the PC was heated to 65 °C, which caused a recovery effect, as previously reported in Refs. [13,15]. The temperature was subsequently lowered again and after six days the measurement was repeated and the photo-current found to be at more than 93% of the level prior to exposure. Other test cathodes showed a recovery of up to 100% of the level before exposure in similar tests. The decrease of QE of the PCs is due to the hydration of the CsI by the adsorbed water molecules and the recovery could be a consequence of the increased desorption of water molecules at higher temperatures.

3.5. Ageing due to ion bombardment

The radiation environment of a HEP experiment continuously causes avalanche processes inside the detector and consequently avalanche ions hitting the CsI layer. This process can decrease the quality of a CsI PC [17,18]. To determine the damage to the detector, a standard PC was irradiated with a colliminated ^{90}Sr beta source inside a detector prototype. The specifications of the experimental procedures used in this ageing test, as well as a discussion of the results are given in Ref. [19]. The VUV-scanner was used to investigate the irradiated PCs. In a first test three positions of approximately 4 cm diameter were irradiated with rather high accumulated charge densities and rates in order to produce a measurable effect. The accumulated charge densities for positions 1, 2, and 3 were of 6.31, 6.79 and 1.54 mC cm^{-2}, respectively,[6] accumulated within 2–9 days. After the irradiation, the PC was re-measured in the scanner. The photo-current scans across the irradiated zones revealed a decreased QE in these zones, as can be seen in Fig. 7. The QE decreases shown in Fig. 7 are close to 80% for positions 1 and 2 and 40% for position 3. In repeated measurements, it was found that the degradation was progressing in time due to a possible self-ageing mechanism [19]. Most recent tests with smaller accumulated charge densities less than 0.2 mC cm^{-2} as well as e.g. the work in Ref. [20] show no such strong ageing effects.

4. Quality monitoring

4.1. Series production

Presently the scanner is mainly used to provide quality monitoring in the ongoing series production of PCs. Immediately, after CsI deposition the photo-current from the PC is monitored to check its development during the heat conditioning phase (see 3.2). Before the PC is extracted from the plant, a scan covering 280 points equally spread over the PC is performed. Usually 6–12% minimum to maximum variation of the normalized current across the PC surface can be measured. Thirty six PCs have been produced and measured since May 2004. The average normalized current $\langle I_{\mathrm{norm}} \rangle$ of the 280-point mappings are used to compare the PC quality. The variation of $\langle I_{\mathrm{norm}} \rangle$ was substantial, with values from 2.7 up to 3.8 corresponding to a spread of almost 33%. This spread was found to be due to a variation in the effectiveness of the heat enhancement (Section 3.2): approximately 20% of all PCs exhibited no enhancement in the initial high temperature phase after CsI deposition. These PCs were either re-coated

[6] 10 years inside ALICE correspond to 0.5 mC cm^{-2}.

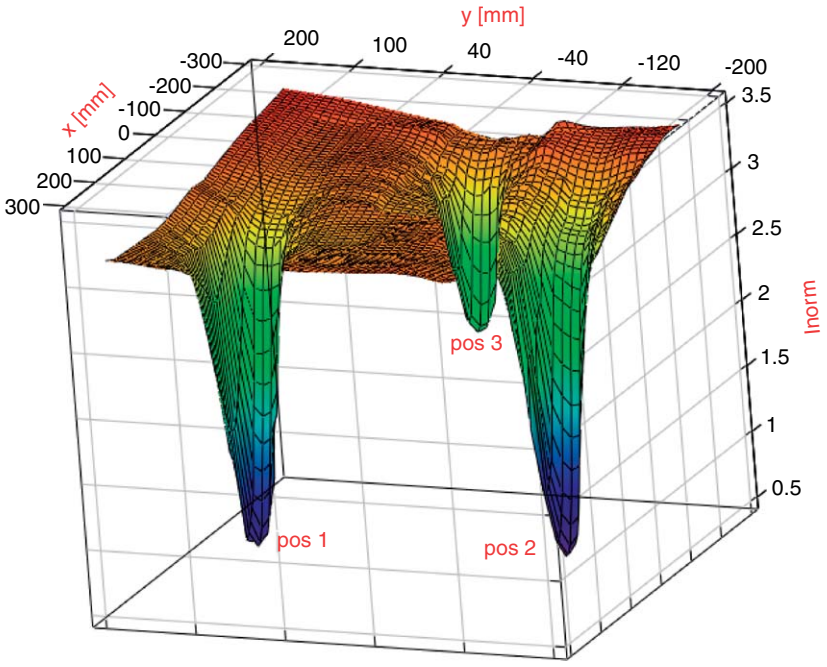

Fig. 7. Scan of the irradiated PC.

showing good results or they showed a delayed enhancement in re-scans weeks or even months after production [21]. In total 33 PCs with values of $\langle I_{\mathrm{norm}}\rangle \geqslant 3$ were accepted for use on the detector. The lower level for acceptance of $\langle I_{\mathrm{norm}}\rangle = 3$ was derived from a comparison of the scans of the first 17 PCs with test beam results as presented in the following section.

4.2. Correlation of scanner and testbeam results

The first seventeen PCs were mounted on three HMPID modules and tested with a 120 GeV/c pion beam [6]. The most important quantity to be measured is the number of resolved clusters per particle track, N_{CL}. This number depends not only on the PC QE, but also on several detector parameters, e.g. radiator transmittance or chamber gain. Therefore, this number can only be used as a first approximation in a direct comparison between test beam and VUV-scanner. Also the differences in photon-flux, spectral composition, and photo-emission have to be kept in mind. In the detector photo-electrons created by single photons are emitted into gas as opposed to a high photon-flux (10^{10} photons $\mathrm{s}^{-1}\,\mathrm{cm}^{-2}$) and photo-emission under vacuum in the scanner. Fig. 8 shows the correlation between N_{CL} and $\langle I_{\mathrm{norm}}\rangle$ at the position of the Cherenkov rings.

The plot also shows the minimum value of $N_{\mathrm{CL}} = 15$, which is required to achieve the necessary Cherenkov angle resolution of 3 mrad. From the first results from the scanner a value of 3 for $\langle I_{\mathrm{norm}}\rangle$ was chosen as the minimum requirement for the PCs, as all the PCs with currents higher than 3 are clearly above the limit for N_{CL}. Despite the general trend visible in Fig. 8 there are some PCs, which performed differently in the test beam than expected from the scanner results, e.g. PC 55. For some of these PCs the differences could be attributed to the delayed enhancement effect mentioned above, as they showed an increased level in later re-scans, e.g. PC 55. Other PCs like PC48 showed a higher level in the scanner in re-scans up to one year after beam tests. To confirm this increase results of currently ongoing cosmic ray tests are awaited. In order to exclude discrepancies due to other detector parameters influencing N_{CL}, an attempt was made to refine the test beam analysis and obtain a quantity more comparable to $\langle I_{\mathrm{norm}}\rangle$. By means of QE($\lambda$) extracted from the test beam data [7] and an estimation of the spectral composition of the photonflux $\Phi(\lambda)$ used in the scanner,[7] the integral

$$I \propto \int_{\lambda} \Phi(\lambda)\cdot \mathrm{QE}(\lambda)\,\mathrm{d}\lambda \tag{1}$$

was calculated, which should be proportional to the photocurrent measured in the scanner. Fig. 9 shows the correlation between this quantity and $\langle I_{\mathrm{norm}}\rangle$ for the PCs for which the QE curves have been calculated.

5. Conclusions

The VUV scanner measurements obtained during the ongoing series production of PCs for the ALICE RICH show that the device is able to provide useful information about the quality of the PCs and the photo-current measurements agree with the test beam results. So far 33

[7] $\Phi(\lambda)$ was obtained by combining the emission characteristics of the UV lamp supplied by the manufacturer with the measured transmittance $T(\lambda)$ of the optical components (lens, windows).

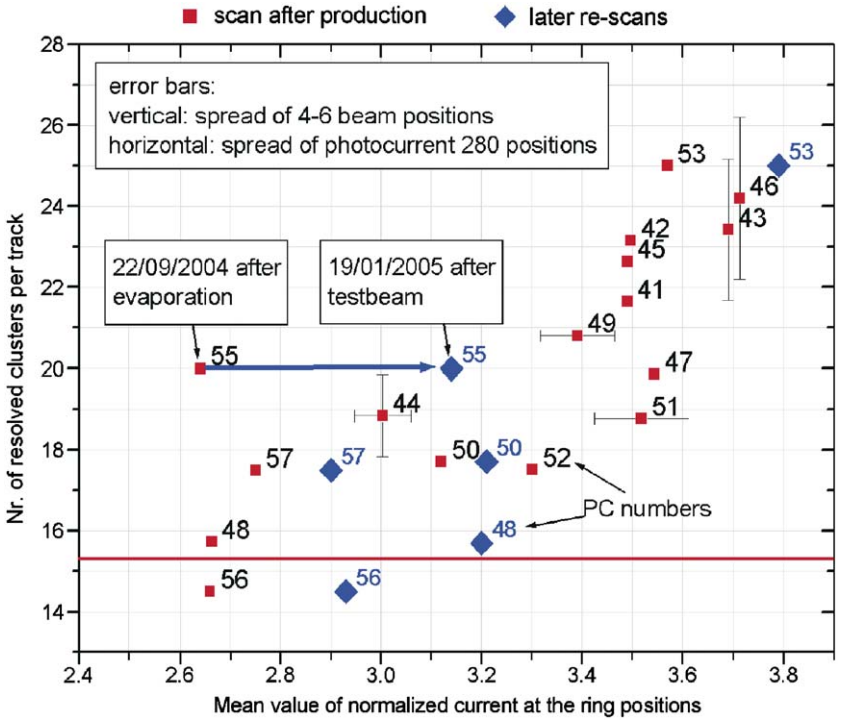

Fig. 8. N_{CL} in the beam plotted against $\langle I_{norm} \rangle$ at the position of the Cherenkov ring.

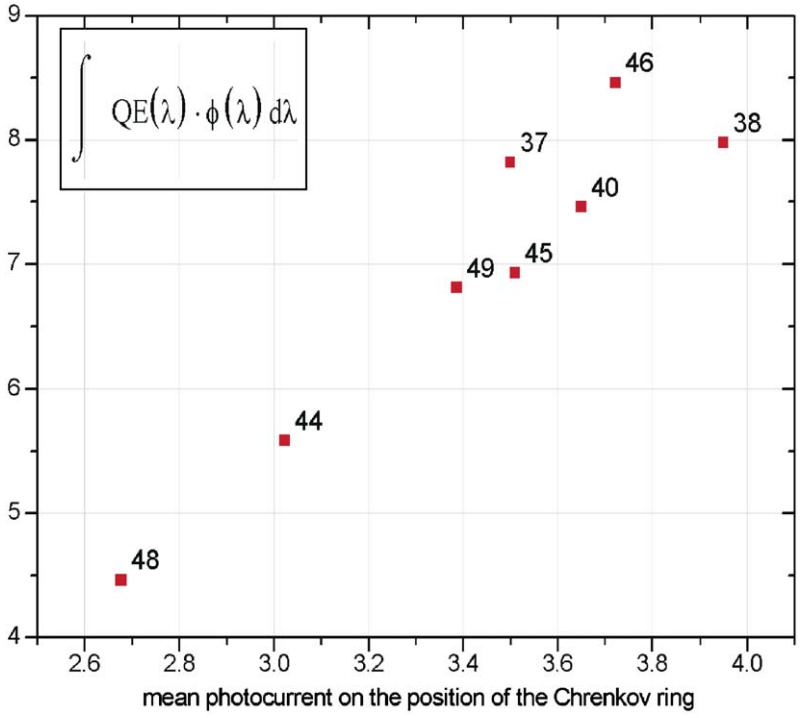

Fig. 9. $\int_{\lambda} \Phi(\lambda) \cdot \mathrm{QE}(\lambda)\, \mathrm{d}\lambda$ from test beam analysis plotted against $\langle I_{norm} \rangle$.

PCs have passed the stringent minimum requirement for the number of resolved clusters in order to achieve the necessary Cherenkov angle resolution for the detector. Furthermore, the device proved to be a versatile research instrument in the study of CsI properties ranging from heat enhancement effects to ageing effects and studies of the influence of the substrate.

Acknowledgments

The operation of the VUV scanner and the production of the PCs relies on the competent support provided by the technical staff at CERN. We would like to thank M. van Stenis, X. Pons, J.B. van Beelen, P. Ijzermans, C. David, M. Malabaila, B. Cantin and D. Fraissard.

References

[1] ALICE collaboration, Physics Performance Report, J. Phys. G 30 (2004) 1517.
[2] ALICE collaboration, ALICE HMPID Technical Design Report, CERN/LHCC 98/19.
[3] A. Braem, et al., Nucl. Instr. and Meth. A 515 (2003) 307.
[4] E. Schyns, Nucl. Instr. and Meth. A 494 (2002) 441.
[5] A. Braem, et al., Nucl. Instr. and Meth. A 502 (2003) 205.
[6] A. Gallas, et al., Nucl. Instr. and Meth. A 553 (2005) 345.
[7] A. Di Mauro, et al., Nucl. Instr. and Meth. A 433 (1999) 190.
[8] H. Hoedlmoser, et al., Nucl. Instr. and Meth. A 553 (2005) 140.
[9] H. Hoedlmoser, CERN-THESIS-2006-004 ⟨http://doc.cern.ch/archive/electronic/cern/preprints/thesis/thesis-2006-004.pdf⟩.
[10] D.F. Anderson, S. Kwan, V. Peskow, B. Hoeneisen, Nucl. Instr. and Meth. A 323 (1992) 626.
[11] A.S. Tremsin, O.H.W. Siegmund, Nucl. Instr. and Meth. A 442 (2000) 337.
[12] A.S. Tremsin, O.H.W. Siegmund, Trans. Nucl. Sci. NS-48 (3) (2001) 421.
[13] Breskin, Nucl. Instr. and Meth. A 371 (1996) 116.
[14] D.F. Anderson, et al., Nucl. Instr. and Meth. A 323 (1992) 626.
[15] H. Brauning, et al., Nucl. Instr. and Meth. A 327 (1993) 369.
[16] J. Va'vra, et al., Nucl. Instr. and Meth. A 387 (1997) 154.
[17] B.K. Singh, et al., Nucl. Instr. and Meth. A 454 (2000) 364.
[18] J. Va'vra, et al., Nucl. Instr. and Meth. A 387 (1997) 154.
[19] A. Braem, et al., Nucl. Instr. and Meth. A 553 (2005) 187.
[20] Z. Fraenkel, et al., Nucl. Instr. and Meth. A 546 (2005) 466.
[21] H. Hoedlmoser, et al., Production technique and quality evaluation of CsI photocathodes for the ALICE/HMPID detector, Nucl. Instr. and Meth. A, 2006, doi:10.1016/j.nima.2006.07.047.